Techno-Economic and Exergetic Evaluation of two-stroke and four-stroke Marine Engines for Onboard Carbon Capture

Diego Díaz-Cuenca[a,b], Antonio Villalba-Herreros[a,b], Teresa J. Leo[a,b] and Rafael d'Amore-Domenech[a,b]

[a] Dept. Arquitectura, Construcción y Sistemas Oceánicos y Navales, ETSI Navales, Universidad Politécnica de Madrid (UPM), Madrid, Spain.
[b] Grupo de Investigación de Pilas de Combustible, Tecnología del Hidrógeno y Motores Alternativos (PiCoHiMA), ETSI Navales, Universidad Politécnica de Madrid (UPM), Madrid, Spain.

Abstract:

This article evaluates the techno-economic, energetic and exergetic suitability of integrating an onboard carbon capture (OCC) system into liquefied natural gas (LNG) propulsed Ro-Ro vessels equipped with either two four-stroke (4T) engines or one two-stroke (2T) engine delivering the same propulsion power. A 30 wt% monoethanolamine (MEA) absorption-regeneration process combined with a Precooled Linde-Hampson (PCLH) CO_2 liquefaction unit was modelled to compare the influence of the engine type on capture performance, waste-heat recovery potential and cost. The assessment was carried out at 85% engine load under consistent design constraints for the capture plant and liquefaction system. Key Performance Indicators (KPIs) included CO_2 avoidance rate, energy consumption, exergy fraction and specific cost of avoided CO_2. The results show that the 2T configuration provides a higher engine exergy efficiency, 53.10% versus 48.39%, due to its lower fuel demand for the same brake power. However, the 4T case offers substantially higher recoverable exhaust heat, 6.440 MW versus 3.060 MW, which improves process integration with the MEA reboiler. As a result, the 4T configuration achieves a higher CO_2 avoidance rate than the 2T engine, 86.4% versus 68.1%, a much lower additional reboiler energy requirement, 0.314 versus 3.002 GJ/tCO_{2AV}. These thermodynamic differences are directly reflected in the economic results, with a specific CO_2 avoided cost of about 74 USD/tCO_{2AV} for the 4T case and 141 USD/tCO_{2AV} for the 2T case. Overall, the study shows that engine selection for OCC should not be based only on propulsion efficiency, but also on the availability and temperature level of recoverable exhaust heat.

Keywords:

Onboard Carbon Capture (OCC); Carbon Capture Storage (CCS); Marine Engines; Energy; Exergy.

1. Introduction

Greenhouse gas (GHG) emissions are a driver of climate change [1]. In 2024, maritime transport accounted for approximately 2.89% of global GHG emissions [2]. To mitigate this impact, the International Maritime Organization (IMO) has established targets to reduce carbon dioxide (CO_2) emissions from shipping by 20% in 2030 and by 70% in 2050 relative to 2008 levels, supported by operational and technical measures such as the Carbon Intensity Indicator (CII) [3], the Energy Efficiency Design Index (EEDI) for new ships [4], and the Energy Efficiency Existing Ship Index (EEXI) for existing ships [5]. At the regional level, the European Union (EU) FuelEU Maritime regulation further strengthens decarbonization efforts by assigning shipowners financial responsibility for the GHG emissions generated by their vessels [6–8]. More recently, at its 83rd session, the IMO Marine Environment Protection Committee (MEPC) approved a work plan for the development of regulations addressing onboard carbon capture (OCC), with completion targeted for 2028 [9].

Among the carbon capture options considered for maritime applications, four main technological pathways can be identified: chemical absorption, physical adsorption, membrane separation, and cryogenic separation. Within these options, amine-based chemical absorption is the most mature and well-established technology, owing to its high capture efficiency and extensive industrial deployment in land-based applications. It is particularly well suited to marine exhaust streams because it can effectively treat flue gases with relatively low CO_2 concentrations, around 4 mol% to 5 mol%, while still achieving a high CO_2 product purity, typically in the range of 95 mol% to 98 mol%. For this reason, amine-based absorption is widely regarded as the reference technology for ship-based carbon capture (SBCC) studies. Nevertheless, one of the main challenges

associated with these systems is their significant thermal energy requirement for solvent regeneration in the stripper (column where the CO_2-rich solution is heated to release absorbed CO_2 and regenerate the absorbent). Consequently, the availability of waste heat on board is a key parameter governing the technical feasibility, energy performance, and overall integration of amine-based carbon capture systems in marine engines [10]. Recent studies on integrated shipboard carbon-capture and waste-heat-recovery systems have likewise shown that flue-gas temperature, flue-gas flow rate, and thermal matching in the heat recovery section strongly affect overall energetic, exergetic, and economic performance [11].

In this context, the main parameters governing the amount of waste heat that can be recovered from a marine engine are the temperature and mass flow rate of the exhaust gas stream. These variables directly determine the thermal energy available for integration with the carbon capture process. In general, the exhaust gas temperature of a four-stroke (4T) marine engine can exceed 300°C, whereas that of a two-stroke (2T) engine is typically in the range of 170 ºC to 200 °C. Nevertheless, despite the clear differences in exhaust-gas thermal conditions between 4T and 2T marine engines, the available literature appears to lack a systematic energetic, exergetic, and techno-economic comparison of these propulsion configurations for onboard carbon capture, particularly with respect to the waste heat available for amine solvent regeneration. Addressing this gap is essential for assessing the feasibility and performance of amine-based OCC across different vessel propulsion systems.

A Ro-Ro vessel was chosen as the case study, since this ship segment provided the most appropriate basis for comparison, allowing the identification of equivalent vessels equipped with different propulsion-system configurations. In addition, both vessels considered are LNG-fueled, reflecting the growing relevance of liquefied natural gas (LNG) as a promising pathway for ship decarbonization. This approach enables a consistent comparison of the influence of engine type on exhaust-gas conditions and on the waste heat potentially available for solvent regeneration. Monoethanolamine (MEA) was selected as the reference solvent because it is the most mature and widely studied option for post-combustion CO_2 capture.

This article is structured as follows. Section 2 presents the methodology, including the definition of the case-study vessel and the two propulsion arrangements, the description of the MEA absorption process, the energetic evaluation of waste heat recovery and carbon capture integration, the exergetic assessment, and the techno-economic analysis. Section 3 reports and discusses the results, while Section 4 provides the main conclusions derived from the work.

2. Methodology

The methodology adopted in this work is summarized in Figure 1. To assess the two propulsion-system configurations, one based on two 4T engines and the other on a single 2T engine, a CO_2 capture system based on MEA was modeled, including a downstream liquefaction stage. In the present case, a pre-cooled Linde–Hampson (PCLH) process was selected, Seo et al. [12] investigated four liquefaction systems and concluded that a PCLH system showed high performance, to enable the cryogenic storage of the captured CO_2. Subsequently, several key performance indicators (KPIs) were analyzed, namely the avoided CO_2 rate, the specific reboiler energy consumption (REC) per unit mass of CO_2, the reboiler exergy fraction (ratio between the exergy carried by the exhaust gases and the fuel exergy input of the engine), and the CO_2 capture cost per unit mass.

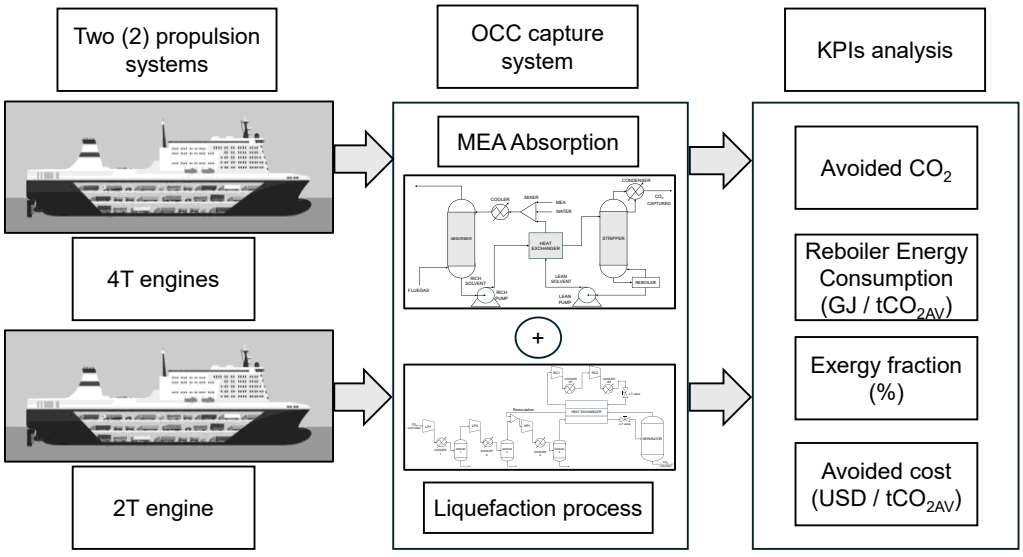

Figure. 1. *Article flowchart.*

All KPIs were calculated under a consistent set of boundary conditions and design assumptions to ensure comparability across OCC configurations. Unless otherwise stated, the capture plant was evaluated at a 90% CO_2 capture rate, justified by the 70% emission reduction target set by the IMO and the 80% reduction required by the FuelEU Maritime regulation. According to the literature, a capture efficiency of around 90% is typically necessary to comply with current international emission reduction standards [13]. Cooling duties were based on the availability of seawater at 25 °C as the heat sink. Heat-exchanger performance was constrained by a maximum temperature approach of approximately 10 °C [14], taken as the minimum allowable hot–cold temperature difference, which limits both heat recovery and the achievable cooling/heating duties.

2.1. Case study vessels propulsion systems

Table 1 summarizes the main dimensions and main characteristics of the vessel. The OCC system is sized at the engine reference operating point, corresponding to 85% of the main engine load. Main engine specifications were obtained using the Computerized Engine Application System (CEAS) [15] under ISO reference conditions, including the exhaust-gas mass flow rate ($\dot{m}_{exh}$), exhaust-gas temperature (T_{exh}), specific fuel oil consumption (SFOC) and specific gas consumption (SGC) [7,16,17]. Methane slip, defined as the release of unburned methane in the exhaust gases due to incomplete combustion or fuel escaping the combustion process, was considered in this work.

Table 1. *Base ships main characteristics and main engine parameters at 85% load.* (*L_{OA}, length overall; L_{PP}, length between perpendiculars; B, beam; D, depth; DWT, deadweight tonnage; SFOC, specific fuel oil consumption; SGC, specific gas consumption*).

Element	4T engine vessel	2T engine vessel	Reference
L_{OA}, m	185.0	185.0	[18]
L_{PP}, m	177.4	177.4	[18]
B, m	25.6	25.6	[18]
D, m	9.2	9.2	[18]
DWT, t	8,702	8,702	[18]
v, m/s	12.1	12.1	[19]
Main Engine	2 x MAN 9L51/60DF (2 x 9,450 kW at 100%)	8S60ME-C10.7-GI (18,900 kW at 100%)	[16,17]
$SFOC$, kJ/kW*h	125	121	[16,17]
SGC, kJ/kW*h	7,025	6,394	[16,17]
Methane slip*, %	3.1	0.2	[7,16,17]
$\dot{m}_{exh}$, kg/s	26.9	35.1	[16,17]
T_{exh}, ºC	334	208	[16,17]
p_{exh}, bar	1.04	1.04	[16,17]

* The methane slip is expressed as a percentage of the total SGC.

Table 2 presents the composition of the exhaust gas for the two propulsion combinations [16,17]. The pilot fuel is assumed to be diesel, resulting in a negligible SO_x concentration. In addition, NO_x emissions from LNG combustion are assumed to be very low and are therefore neglected in this study.

Table 2. *Exhaust gas composition* (*mol%, percentage in molar basis*).

Element	4T engine vessel	2T engine vessel	Reference
CO_2, mol%	4.2873	3.1123	[16,17]
N_2, mol%	73.9912	74.9879	[16,17]
O_2, mol%	11.4189	14.0239	[16,17]
H_2O, mol%	9.2881	6.9763	[16,17]
Ar, mol%	0.8818	0.8936	[16,17]
CH_4, mol%	0.1328	0.0060	[16,17]

The fuel properties [4,20–22] are presented in Table 3.

Table 3. *Fuels properties.* (*LHV, lower heating value; ρ, density; c_f, carbon content of the fuel; β, is the fuel-dependent exergy coefficient defined as the ratio of the fuel chemical exergy to its lower heating value*).

Element	LNG	Diesel	Reference
LHV, MJ/kg	48.00	42.70	[4]
ρ, kg/m^3	460	900	[22]
c_f, m_{CO_2}/m_{fuel}	2.750	3.206	[4]
β	1.04	1.07	[20,21]

2.2. MEA Absorption

The selected amine for this work is monoethanolamine (MEA), which is widely regarded as the benchmark solvent for post-combustion CO_2 capture. MEA is a primary ethanolamine that can be protonated to form the cation $MEAH^+$ and can react with CO_2 to form carbamate species, represented as $MEACOO^-$ [23]. Owing to its fast absorption kinetics and proven performance, a 30 wt% aqueous MEA solution remains the standard solvent for chemical absorption and is therefore adopted as the reference case in this study. This solvent solution is the most commercially established amine technology, supported by extensive pilot and industrial experience, with well-characterized performance, degradation pathways, and operating practices. Its maturity and broad availability make it a reliable reference solvent for comparative assessments and for evaluating alternative capture options and shipboard integration strategies [24].

Figure 2 shows a conventional MEA-based post-combustion CO_2 absorption/regeneration loop. Flue gas enters the absorber, where CO_2 is chemically absorbed by the aqueous amine solution, producing a cleaned gas stream leaving the top of the column and a CO_2-rich solvent (rich solvent) leaving the bottom. The rich solvent is pumped through a lean/rich heat exchanger, where it is preheated by the returning regenerated solvent, improving overall thermal efficiency, and then fed to the stripper (desorber). In the stripper, heat supplied by the reboiler reverses the absorption reaction and releases concentrated CO_2; the overhead vapor passes through a condenser to remove water and recover solvent, while the CO_2 product stream exits as captured CO_2. The regenerated lean solvent is cooled (via the cooler), returned through the heat exchanger, and pumped back to the absorber to close the loop. A mixer/make-up line is included to maintain solvent composition (amine and water) and compensate for losses or degradation.

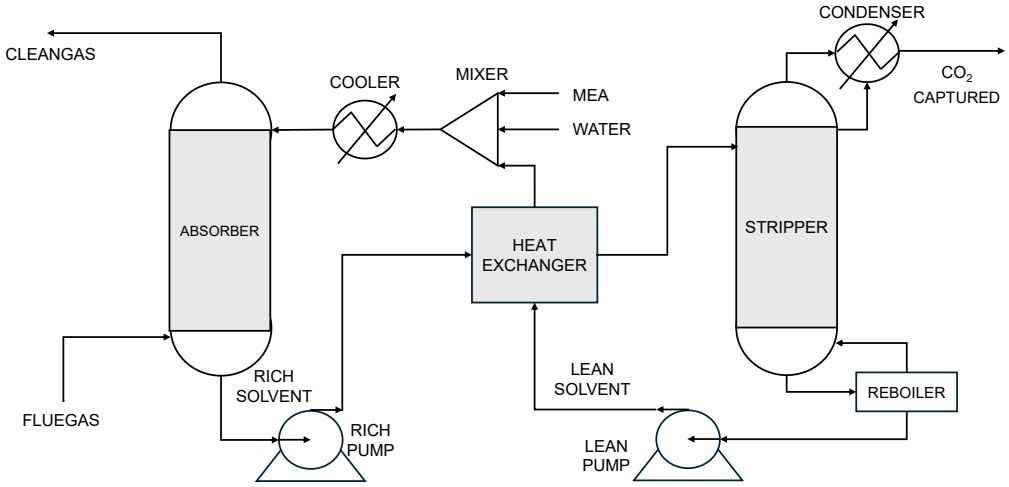

Figure. 2. *Schematic of the MEA Absorption–Regeneration Process for Post-Combustion CO_2 Capture.* (*MEA, monoethanolamine*) [14].

Table 4 presents the main assumptions for the construction of the MEA absorption process. For both absorption and stripping columns, Mellapak 350X packing was selected. A maximum flooding rate of 80% was imposed for both the absorber and the stripper. In addition, the reboiler pressure was selected to ensure that the operating temperature does not exceed 120 °C, the threshold above which MEA degradation may occur.

Table 4. *Main Assumptions of the MEA absorption process for both propulsion systems.*

Element	Value	Reference
Base method	ELECNRTL	[25]
Packing Type	Mellapak 350X	-
Max. *T* at the reboiler, ºC	120	[23]
Max. Absorber Height, m	12.0	-
Max. Absorber Diameter, m	4.0	-
Max. Stripper Height, m	12.0	-
Max. Stripper Diameter, m	4.0	-
Max. Flooding Rate, %	80	[14]

2.3. Liquefaction system

The precooled Linde-Hampson (PCLH) cycle is selected as the reference CO_2 liquefaction process in this work, and the corresponding scheme is shown in Figure 3. PCLH is widely adopted due to its simple layout, low flow resistance, and ease of control, and recent thermodynamic studies report robust energy and exergy

performance, with precooling improving liquid yield and efficiency compared with the basic Linde-Hampson configuration [26]. In techno economic assessments of CO_2 shipping chains, PCLH achieves liquefaction costs comparable to leading vapor compression options while typically requiring lower total capital expenditure, supporting its suitability for onboard applications [27]. Process simulation and equipment sizing are carried out using the Peng-Robinson equation of state [28] to ensure consistent property prediction in near critical and subcooled regions, and ammonia (NH_3) is selected as the refrigerant for the precooling vapor compression loop, operating with evaporating temperatures from -10 °C to -40 °C, 2 bar to 6 bar and water cooled condensing temperatures of 30 °C [12]. Shipboard CO_2 storage conditions are set to 16 bar and -26 °C, consistent with demonstrated onboard practice and close to the techno economic optimum reported in the literature for marine CO_2 transport [27,29].

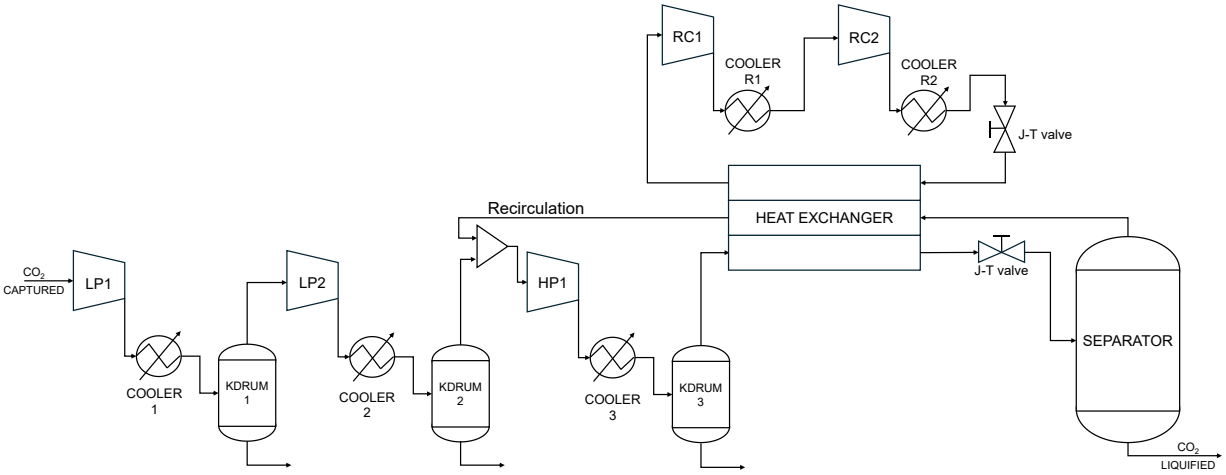

Figure. 3. *Precooled Linde–Hampson CO_2 liquefaction process with NH_3 vapor compression precooling* (*J-T, Joule-Thomson valve*) [12].

2.4. Avoided CO_2

Total CO_2 includes emissions from the main engine plus additional emissions from OCC utilities: auxiliary boiler (steam for regeneration), power generation (electricity for pumps/compressors), and cooling-water pumping (treated as extra electrical load). Utility emissions are assumed supplied by MGO:

$$\dot{m}_{CO_{2U}} = (\dot{m}_{Boiler} SFOC_{Boiler} + \dot{m}_{Gen} SFOC_{Gen}) C_f, \tag{1}$$

where the $\dot{m}_{CO_{2U}}$ represents the mass flow rate CO_2 emitted by the carbon capture system; $\dot{m}_{Boiler}$ is the fuel mass flow rate to the auxiliary boiler; $SFOC_{Boiler}$ is the specific fuel oil consumption of the boiler; $\dot{m}_{Gen}$ is the fuel mass flow rate to the generator engine; $SFOC_{Gen}$ is the specific fuel oil consumption of the generator engine; and C_f is the carbon factor of MGO.

The efficiency assumptions and specific fuel oil consumption values adopted for the auxiliary systems, namely a boiler efficiency of 95% [30], an alternator efficiency of 95%, a $SFOC$ consumption of 55.7 kg Diesel per t of steam for the boiler [30], and 48.6 kg per GJ for power generation [31].

Avoided metrics are:

$$\dot{m}_{CO_{2AV}} = \dot{m}_{CO_{2CAP}} - \dot{m}_{CO_{2U.Boiler}} - \dot{m}_{CO_{2U.Gen}}, \tag{2}$$

$$\mathrm{CO_{2AV.R}} = \frac{\dot{m}_{CO_{2AV}}}{\dot{m}_{CO_{2ME}}} \cdot 100, \tag{3}$$

where $\dot{m}_{CO_{2AV}}$ represents the amount of CO_2 avoided from being emitted to the atmosphere; $\dot{m}_{CO_{2CAP}}$ is the CO_2 captured by the SBCC system; $\dot{m}_{CO_{2ME}}$ is the CO_2 emitted by the main engine; $\mathrm{CO_{2CAP.R}}$ and $\mathrm{CO_{2AV.R}}$ are the capture and avoided rate, respectively; $\dot{m}_{CO_{2U.Boiler}}$ and $\dot{m}_{CO_{2U.Gen}}$ represent the CO_2 emitted by the boiler and the electric generators of the capture system, respectively.

2.5. Energetic analysis

The energetic performance is evaluated using the brake thermal efficiency and the recoverable exhaust heat that can be transferred to a waste-heat recovery unit (WHRU) while meeting the temperature requirements imposed by amine-based solvent regeneration. The brake thermal efficiency is defined as:

$$\eta_{th} = \frac{\dot{W}_b}{\dot{m}_{f_{LNG}} \cdot \mathrm{LHV}_{LNG} + \dot{m}_{f_{Diesel}} \cdot \mathrm{LHV}_{Diesel}}, \tag{4}$$

where $\dot{W}_b$ is the brake power; $\dot{m}_{f_{LNG}}$ is the fuel mass flow rate of LNG; $\dot{m}_{f_{Diesel}}$ is the fuel mass flow rate of diesel; LHV_{LNG} is the lower heating value of LNG and LHV_{Diesel} is the lower heating value of diesel.

The available exhaust-gas thermal power from the waste heat recovery unit (WHRU), denoted ($\dot{Q}_{WHRU}$), was evaluated in REFPROP 9.1 [32] by modelling the exhaust cooling process from the WHRU inlet conditions down to 135 °C (T_{out}). The exhaust outlet temperature is not arbitrarily selected; instead, it is constrained by the requirement to produce saturated steam at approximately 120 ºC for the reboiler. Accordingly, T_{out} is limited to values not lower than T_{steam} plus ΔT_{min}, and, when considered, an additional minimum stack temperature may be imposed to avoid low-temperature corrosion. The waste heat is calculated as:

$$\dot{Q}_{WHRU} = \eta_{WHRU} \cdot \dot{m}_{exh} \cdot [h(T_{exh}, p) - h(T_{out}, p)], \quad (5)$$

where $\dot{Q}_{WHRU}$ is the useful heat rate that can be extracted from the exhaust stream; η_{WHRU} is the efficiency of the WHRU, in this case 90%; $\dot{m}_{exh}$ represents the mass flow rate of the exhaust gas; $h(T_{out}, p)$ is the specific enthalpy of the exhaust gas at the WHRU outlet temperature T_{out} and pressure p; $h(T_{exh}, p)$ specific enthalpy of the exhaust gas at the WHRU inlet/exhaust temperature T_{exh} and pressure p; T_{exh} is the exhaust gas temperature at WHRU inlet; T_{out} is the exhaust gas temperature at WHRU outlet and p exhaust-gas pressure at which the enthalpies are evaluated.

Therefore, the reboiler energy consumption (REC) is the indicator that quantifies the amount of energy consumed by the system per unit mass of CO_2, and it is calculated as:

$$REC_{AV} = \frac{\dot{Q}_{REB} - \dot{Q}_{WHRU}}{\dot{m}_{CO_{2AV}}}, \quad (6)$$

where REC_{AV} is the reboiler energy consumption per unit of CO_2 mass; $\dot{Q}_{REB}$ is the reboiler energy consumption; $\dot{Q}_{WHRU}$ is the is the useful heat rate that can be extracted from the exhaust stream and $\dot{m}_{CO_{2AV}}$ is the avoided CO_2 mass flow rate.

2.6. Exergetic analysis

The exergetic assessment complements the energy analysis by quantifying not only the magnitude of energy flows, but also their thermodynamic quality relative to a reference environment [33]. In this study, total exergy is evaluated with respect to the dead state, defined as the condition of complete thermodynamic equilibrium between the system and the environment. This state is specified by the ambient temperature T_0, ambient pressure p_0, and the chemical composition of the surroundings; here, T_0 is 298.15 K and p_0 is 1 atm. By definition, a system at the dead state is in thermal, mechanical, and chemical equilibrium with the environment and therefore has zero exergy [34]. Accordingly, the exergy values reported in this study represent the maximum theoretical useful work obtainable as the considered stream or system is brought reversibly to the dead state.

Within this framework, the exergy of a material stream is decomposed into physical and chemical contributions:

$$ex = ex^{ph} + ex^{ch}, \quad (7)$$

where ex is the total exergy; ex^{ph} is the physical exergy and ex^{ch} is the chemical exergy.

The physical exergy, which is the dominant contribution for hot exhaust gases in waste-heat recovery applications, accounts for the departure of the stream temperature and pressure from the dead state and is expressed as:

$$ex^{ph} = (h - h_0) - T_0(s - s_0), \quad (8)$$

where h and s are the specific enthalpy and entropy, respectively, at the stream conditions, and h_0 and s_0 are evaluated for the same stream composition at T_0 and p_0.

The fuel chemical exergy was estimated using the classical approximation proposed in the exergy literature, in which the specific chemical exergy is related to the LHV through a fuel-dependent coefficient, β [35–37]. The fuel exergy rate is therefore approximated as:

$$\dot{E}x_{fuel} = \dot{m}_{f_{LNG}} \cdot \beta_{LNG} \cdot LHV_{LNG} + \dot{m}_{f_{Diesel}} \cdot \beta_{Diesel} \cdot LHV_{Diesel}, \quad (9)$$

where $\dot{E}x_{fuel}$ is the fuel exergy rate; $\dot{m}_{f_{LNG}}$ is the fuel mass flow rate of LNG; $\dot{m}_{f_{Diesel}}$ is the fuel mass flow rate of diesel; β_{LNG} is the fuel-dependent factor for the LNG, taken as 1.04 [21]; β_{Diesel} is the fuel-dependent factor for the diesel, taken as 1.07 [20]; LHV_{LNG} is the lower heating value of LNG and LHV_{Diesel} is the lower heating value of diesel.

The overall engine exergy efficiency is calculated in Eq. (10). providing a measure of the fraction of the fuel useful potential converted into brake power once irreversibilities are accounted for.

$$\eta_{ex,eng} = \frac{\dot{W}_b}{\dot{E}x_{fuel}}, \quad (10)$$

where $\eta_{ex,eng}$ is the overall engine exergy fraction; $\dot{W}_b$ is the brake power and $\dot{E}x_{fuel}$ is the fuel exergy rate.

To directly relate exhaust-gas heat recovery to the amine regeneration requirement, the potential associated with heat supplied at the reboiler temperature level is quantified through the exergy of heat transfer. When a heat rate $\dot{Q}_{WHRU}$ is delivered at an effective boundary temperature T_b, its associated exergy rate is:

$$\dot{E}x_Q = \left(1 - \frac{T_0}{T_b}\right)\dot{Q}_{WHRU}, \quad (11)$$

where $\dot{E}x_Q$ is the exergy of the heat rate; T_0 is the ambient temperature; T_b is the boundary temperature and $\dot{Q}_{WHRU}$ is the waste heat recovery heat.

In this application, T_b is taken as the saturation temperature of the reboiler steam (T_{steam}), which defines the temperature level at which the regeneration energy is supplied and, therefore, determines the corresponding exergy content of the recovered heat:

$$\dot{E}x_{reb} = \left(1 - \frac{T_0}{T_{steam}}\right)\dot{Q}_{WHRU}, \quad (12)$$

where $\dot{E}x_{reb}$ is the reboiler exergy; T_0 is the ambient temperature; T_{steam} is the saturation temperature of the reboiler steam and $\dot{Q}_{WHRU}$ is the waste heat recovery heat. the reboiler exergy fraction, defined as the ratio between the exergy associated with the heat recovered for solvent regeneration at the reboiler temperature level and the fuel exergy input of the engine:

$$\psi_{reb} = \frac{\dot{E}x_{reb}}{\dot{E}x_{fuel}}, \quad (13)$$

where ψ_{reb} is the reboiler exergy fraction; $\dot{E}x_{reb}$ is the reboiler exergy and $\dot{E}x_{fuel}$ is the exergy of the fuel.

This indicator is particularly suitable for comparing 2T and 4T cases, because the exhaust temperature level strongly influences both the recoverable WHRU duty under pinch constraints and the corresponding exergy content of the delivered regeneration heat.

2.7. Economic analysis

The economic component is divided into Capital Expenditures (CAPEX), Variable Operating Expenditures (VOPEX), and Fixed Operating Expenditures (FOPEX). The CAPEX was developed using a bottom-up approach aligned with the framework proposed. Direct equipment costs for all major items were obtained from Aspen Process Economic Analyzer (APEA v12.1) [38] using the specified materials, design pressures/temperatures, and energy consumption; items not native to APEA were scaled to the required capacity and normalized to a common price year. These line items were summed to the Total Direct Cost (TDC), to which a process contingency of 10% of TDC was added, yielding the Total Direct Cost including Process Contingency (TDCPC). Indirect costs equal to 15% of TDCPC were then included to form the Engineering, Procurement and Construction (EPC) cost. A project contingency of 30% of EPC was applied and combined with EPC to give the Total Plant Cost (TPC). The owner costs were taken as 7.5% of TPC and the resulting subtotal was escalated with discount rate, plus start-up costs, to obtain the Total Capital Requirement (TCR) reported in this work. The annual FOPEX includes maintenance, insurance and taxes and has been set as 5% of the TPC. Regarding VOPEX, Table 5 presents a breakdown of the utilities economic costs. The CO_2 avoided cost is calculated as:

$$Cost(CO_{2AV}) = \frac{Annualized\ CAPEX + Annual\ VOPEX + Annual\ FOPEX}{Annual\ CO_2\ avoided}, \quad (14)$$

where $Cost(CO_{2AV})$ is the annualized cost per unit of mass of CO_2 avoided.

Table 5. *Utilities economic costs* (*SFOC; Specific Fuel Oil Consumption*).

Element	Value	Reference
Boiler Efficiency, %	95.0	[30]
Alternator Efficiency, %	95.0	-
$SFOC_{Boiler}$, kgMGO/tSteam	55.7	[30]
$SFOC_{Gen}$, kg/GJ	48.7	[31]
MGO cost, USD/t	663.0	[39]
Steam cost, USD/t	39.78	-
Electricity cost, USD/kW*h	0.123	-

3. Results and discussion

The results are organized into three sections. Section 3.1 presents the characteristics of the capture systems, together with the amounts of CO_2 captured and avoided. Section 3.2 reports the results of the energy and exergy analyses. Finally, Section 3.3 presents the results of the economic analysis.

3.1. Capture system parameters

Table 6 presents the results obtained after optimizing the reboiler energy consumption. In the case of the absorber, the maximum dimensions considered geometrically acceptable for installation on board the vessel were reached in both cases. For the stripper, in the 4T engine case, a diameter of 1.5 and a height of 9.3 were obtained, whereas for the 2T engine case, a diameter of 1.6 and a height of 10.9 were obtained. The solvent flow rate is of similar magnitude in both configurations, being 43.5 kg/s for the 4T engine and 41.5 kg/s for the 2T engine, while the reflux ratio is slightly higher for the 2T case, 1.502 versus 1.422. The table also shows differences in the CO_2 capture performance between the two engine configurations. The calculated CO_2 avoidance rate is 86.4% for the 4T engine and 68.1% for the 2T engine. This difference can be associated with the different amounts of thermal energy recovered in the WHRU, which is higher in the 4T case. Since solvent regeneration in an MEA process is strongly dependent on heat availability, the higher waste heat in the 4T configuration supports a higher regeneration capability and, consequently, a higher CO_2 avoidance rate. Overall, the results indicate that, while the main absorption-regeneration layout remains similar in both cases, the level of waste heat available for process integration has a noticeable influence on the system performance.

Table 6. *Comparison of key design parameters and CO_2 capture performance of the MEA absorption system for vessels equipped with 4T and 2T engines ($\dot{m}_{CO_{2AV}}$ represents the amount of CO_2 avoided from being emitted to the atmosphere; $\dot{m}_{CO_{2CAP}}$ is the CO_2 captured by the SBCC system; $CO_{2CAP.R}$ is the avoided rate; $\dot{m}_{CO_{2U.Boiler}}$ and $\dot{m}_{CO_{2U.Gen}}$ represents the CO_2 emitted by the boiler and the electric generators of the capture system respectively).*

Element	4T engine	2T engine
Absorber Height, m	12.0	12.0
Absorber Diameter, m	4.0	4.0
Stripper Height, m	9.3	10.9
Stripper Diameter, m	1.5	1.6
Solvent flow, kg/s	43.5	41.5
Reflux ratio, mol/mol	1.422	1.502
$\dot{m}_{CO_{2U.Boiler}}$, kg/h	129.4	976.0
$\dot{m}_{CO_{2U.Gen}}$, kg/h	104.1	100.0
$\dot{m}_{CO_{2CAP}}$, kg/h	5809.7	5469.5
$\dot{m}_{CO_{2AV}}$, kg/h	5576.3	4393.5
$CO_{2AV.R}$, %	86.4	68.1

3.2. Energetic and Exergetic analysis

Table 7 evidences a clear tradeoff between propulsion conversion performance and the ability to supply amine regeneration heat exclusively from recovered exhaust energy under the imposed steam temperature constraint. For the same delivered power output, 16.065 MW, the 2T case requires a lower fuel exergy input than the 4T case, 30.252 MW versus 33.200 MW, which directly yields a higher overall engine exergy efficiency, 53.10%, for the 2T compared to 48.39% for the 4T. This indicates that, at the investigated operating condition, the 2T configuration converts a larger fraction of the fuel into propulsion work and therefore presents a lower intrinsic irreversibility per unit delivered power, which is consistent with its lower $\dot{E}x_{fuel}$ requirement for the same $\dot{W}_b$.

In contrast, the exhaust heat recovery results show that the 4T configuration provides substantially higher recoverable thermal power to the WHRU, 6.440 MW compared to 3.060 MW for the 2T, which is consistent with the higher exhaust temperature level assumed for the 4T and the larger permissible exhaust cooling range while maintaining the minimum outlet temperature required to generate saturated steam at 120 ºC with a finite approach temperature. When this recovered heat is expressed as exergy terms at the reboiler temperature level, the corresponding regeneration heat exergy is 1.556 MW for the 4T and 0.739 MW for the 2T. The resulting reboiler exergy fraction, ψ_{reb}, highlights the different levels of thermodynamic “enabling capacity” for solvent regeneration, with 4.69% of the fuel exergy being convertible into reboiler grade heat in the 4T case compared to 2.44% in the 2T case, indicating that the 4T configuration can route almost twice the useful potential of the fuel toward regeneration through exhaust recovery.

This difference is directly reflected in the REC_{AV} indicator, which in this study represents the additional heat requirement per avoided CO_2 beyond what can be supplied by the WHRU. Because $\dot{Q}_{WHRU}$ in the 4T case is close to the regeneration demand, the required supplemental heat is small, yielding 0.314 GJ/tCO_2 avoided, whereas the 2T case, limited by a substantially lower recoverable exhaust energy under the same steam constraint, exhibits a larger regeneration heat deficit and therefore a markedly higher 3.002 GJ/tCO_2 avoided. Overall, the results demonstrate that selecting a propulsion architecture for onboard carbon capture cannot be based solely on engine efficiency metrics, as the 2T case is favorable from a propulsion exergy efficiency perspective, while the 4T case is favorable from an integration perspective. The 4T higher exhaust heat availability at usable temperature levels minimizes the need for external regeneration heat and improves the thermodynamic viability of an exhaust only amine regeneration strategy.

Table 7. *Energy and exergy performance indicators for the 4T and 2T propulsion cases, including WHRU heat recovery and reboiler-grade exergy available for amine regeneration ($\dot{W}_b$, brake power; $\dot{Q}_{WHRU}$, waste heat; REC_{AV}, Reboiler energy consumption per mass of CO_2 avoided; $\dot{E}x_{fuel}$, fuel exergy; $\eta_{ex,eng}$, exergetic efficiency of the engine; $\dot{E}x_Q$, reboiler exergy; ψ_{reb}, reboiler exergy fraction*).

Element	4T engine	2T engine
$\dot{W}_b$, MW	16.065	16.065
$\dot{Q}_{WHRU}$, MW	6.440	3.060
REC_{AV}, GJ/tCO_{2AV}	0.314	3.002
$\dot{E}x_{fuel}$, MW	33.200	30.252
$\eta_{ex,eng}$, %	48.39	53.10
$\dot{E}x_{reb}$, MW	1.556	0.739
ψ_{reb}, %	4.69	2.44

3.3. Economic analysis

Figure 4 presents the specific cost of $\dot{m}_{CO_{2AV}}$, expressed in USD/tCO_{2AV}, for the onboard capture system applied to 4T and 2T marine engines, together with its breakdown into capital and operating cost components. In both cases, the total cost is obtained by summing the contributions from the CO_2 capture unit, SBCC, and the liquefaction section.

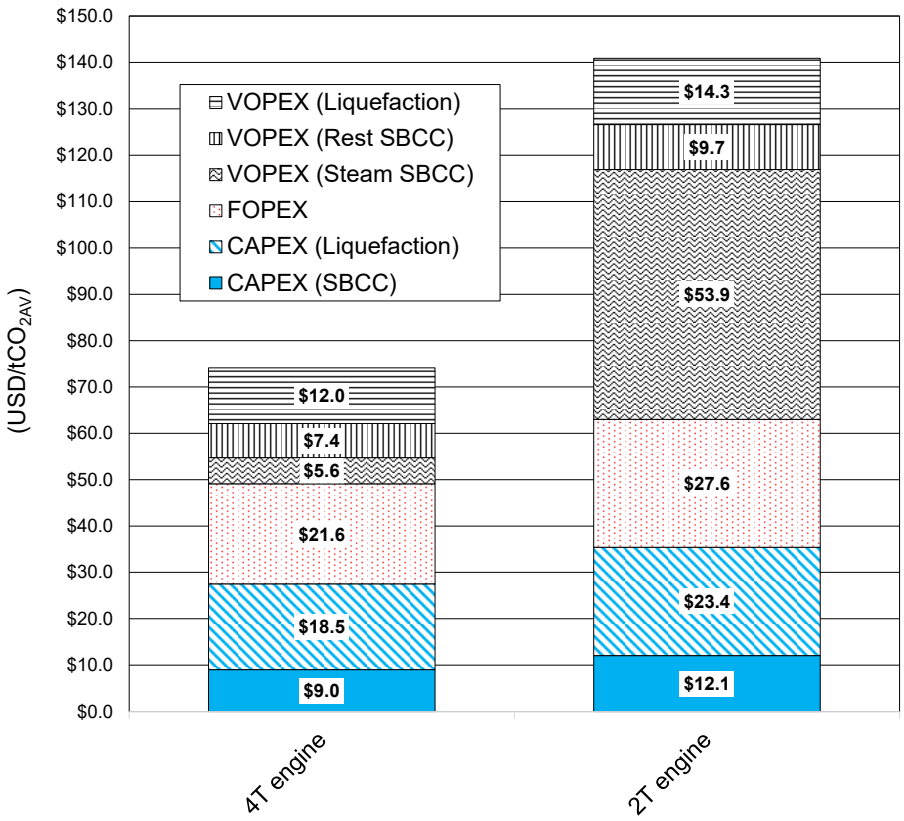

Figure. 4. *Breakdown of the specific CO_2 avoidance cost for onboard capture in 4T and 2T marine engines.*

For the 4T engine, the total specific avoidance cost is approximately 74 USD/tCO_{2AV}. The main contributions are FOPEX, 21.6 USD/tCO_{2AV}, and CAPEX of the liquefaction unit, 18.5 USD/tCO_{2AV}, followed by VOPEX associated with liquefaction, 12.0 USD/tCO_{2AV}, CAPEX of the SBCC unit, 9.0 USD/tCO_{2AV}, VOPEX of the rest of the SBCC system, 7.4 USD/tCO_{2AV}, and VOPEX related to steam consumption in the SBCC, 5.6 USD/tCO_{2AV}. For the 2T engine, the total specific avoidance cost increases to approximately 141 USD/tCO_{2AV}, which is almost twice the value obtained for the 4T case. In this configuration, the dominant contribution is VOPEX associated with steam consumption in the SBCC, 53.9 USD/tCO_{2AV}. The other relevant components are FOPEX, 27.6 USD/tCO_{2AV}, CAPEX of the liquefaction unit, 23.4 USD/tCO_{2AV}, VOPEX of liquefaction, 14.3 USD/tCO_{2AV}, CAPEX of the SBCC unit, 12.1 USD/tCO_{2AV}, and VOPEX of the rest of the SBCC system, 9.7 USD/tCO_{2AV}. Overall, the figure shows that the 2T engine configuration is associated with a significantly higher CO_2 avoidance cost than the 4T configuration. The most evident difference lies in the steam-related variable operating cost of the SBCC unit, which becomes the largest single cost item in the 2T case, whereas in the 4T case the cost contributions are more evenly distributed among fixed operating cost, liquefaction CAPEX, and the remaining cost categories. Thus, the figure indicates that the cost gap between the two engine options is primarily driven by the operating cost of the capture process, while capital-related contributions increase more moderately.

4. Conclusions

This article presents an energy, exergy, and techno-economic assessment of an onboard carbon capture system for a Ro-Ro vessel, comparing two possible propulsion system configurations: the first based on two four-stroke (4T) engines and the second on a single two-stroke (2T) engine. The capture system was based on an amine absorption process, specifically monoethanolamine (MEA), with a downstream Precooled Linde-Hampson (PCLH) liquefaction system.

For the same delivered brake power, the 2T propulsion configuration shows the best standalone propulsion performance. The 2T case requires a lower fuel exergy input, 30.252 MW versus 33.200 MW for the 4T case, and therefore reaches a higher engine exergy efficiency, 53.10% compared with 48.39%. From a propulsion-only perspective, the 2T engine is therefore the more efficient solution.

However, the 4T configuration is clearly more favorable for integration with the onboard monoethanolamine (MEA) capture process because it provides substantially more recoverable exhaust heat. The 4T case delivers 6.440 MW of waste heat versus 3.060 MW for the 2T case, which translates into a higher reboiler-grade exergy, 1.556 MW versus 0.739 MW, and a larger reboiler exergy fraction, 4.69% versus 2.44%. Therefore, the 4T case reaches a much lower additional reboiler energy requirement, 0.314 GJ/tCO_{2AV} compared with 3.002 GJ/tCO_{2AV}, and a higher CO_2 avoidance rate, 86.4% versus 68.1%. These results show that the availability of useful waste heat is a decisive factor in the performance of ship-based MEA capture.

The techno-economic results follow the same trend. The specific CO_2 avoidance cost is about 74 USD/tCO_{2AV} for the 4T engine and 141 USD/tCO_{2AV} for the 2T engine, which is approximately 90% higher than for the 4T engine. The largest difference is associated with steam-related variable operating costs, which become the dominant cost contribution in the 2T case because of its lower exhaust heat recovery potential.

Overall, the study supports the conclusion that selecting a propulsion architecture for onboard carbon capture (OCC) should not be based only on engine efficiency. For this application, the 4T solution is less favorable as a prime mover alone, but more favorable as an integrated propulsion-capture system because its exhaust conditions reduce the external regeneration heat demand and improve both the energetic and economic performance of the OCC plant.

Acknowledgements

The authors acknowledge the Spanish Ministry of Science and Innovation through the State Agency for Research and European Regional Development Funds through the Research Project PID2021-124263OB-I00 funded by MCIN/AEI/ 10.13039/501100011033 and by “ERDF a way of making Europe”. The authors also acknowledge the Spanish Ministry of Science and Innovation through the “NextGenerationEU/PRTR” and the Regional Government of Madrid through the Research Project GreenH2CM funded by MCIU/AEI/10.13039/501100011033.

References

[1] Sun R, Abouarghoub W, Demir E, Potter A. A comprehensive analysis of strategies for reducing GHG emissions in maritime ports. Mar Policy 2025;171. https://doi.org/10.1016/j.marpol.2024.106455.

[2] IMO. Review Maritime Transport 2024. 2024.

[3] IMO. Resolution MEPC.336(76). Guidelines on operational carbon intensity indicators and the calculation methods (CII). 2021.

[4] IMO. Resolution MEPC.364(79). Guidelines on the method of calculation of the attained energy efficiency design index (EEDI) for new ships. 2022.

[5] IMO. Resolution MEPC.333(76). Guidelines on the method of calculation of the attained energy efficiency existing index (EEXI). 2021.

[6] Erbach G, Jensen L. Fit for 55 package. EPRS, European Parliament 2022.

[7] EU. Regulation (EU) 2023/1805 of the European Parliament and of the Council of 13 September 2023 on the use of renewable and low-carbon fuels in maritime transport, and amending Directive 2009/16/EC. 2023.

[8] Oh J, Kim D, Roussanaly S, Lim Y. Greenhouse gas emissions of shipping with onboard carbon capture under the FuelEU Maritime regulation: A well-to-wake evaluation of different propulsion scenarios. Chemical Engineering Journal 2024;498. https://doi.org/10.1016/j.cej.2024.155407.

[9] Vakili S, Manias P, Turnock S, Teagle D. Techno-economic and environmental assessment of Onboard Carbon Capture for maritime net-zero compliance. J Environ Manage 2025;395. https://doi.org/10.1016/j.jenvman.2025.127677.

[10] Díaz-Secades LA, González R, Rivera N. Waste heat recovery from marine engines and their limiting factors: Bibliometric analysis and further systematic review. Cleaner Energy Systems 2023;6. https://doi.org/10.1016/j.cles.2023.100083.

[11] Zhang Y, Zhang J, Tian Z, Yang C, Peng H, Kan A, et al. Comparative analysis of coupled carbon capture and waste heat recovery systems for ships using the 5E approach. Energy Convers Manag 2025;326. https://doi.org/10.1016/j.enconman.2024.119454.

[12] Seo Y, Huh C, Lee S, Chang D. Comparison of CO2 liquefaction pressures for ship-based carbon capture and storage (CCS) chain. International Journal of Greenhouse Gas Control 2016;52:1–12. https://doi.org/10.1016/j.ijggc.2016.06.011.

[13] Feenstra M, Monteiro J, van den Akker JT, Abu-Zahra MRM, Gilling E, Goetheer E. Ship-based carbon capture onboard of diesel or LNG-fuelled ships. International Journal of Greenhouse Gas Control 2019;85:1–10. https://doi.org/10.1016/j.ijggc.2019.03.008.

[14] Ros JA, Skylogianni E, Doedée V, van den Akker JT, Vredeveldt AW, Linders MJG, et al. Advancements in ship-based carbon capture technology on board of LNG-fuelled ships. International Journal of Greenhouse Gas Control 2022;114. https://doi.org/10.1016/j.ijggc.2021.103575.

[15] Everllence. CEAS engine calculations 2026.

[16] Everllence. MAN 51/60DF Project Guide – Marine Four-stroke dual fuel engine compliant with IMO Tier II/IMO Tier III. 2024.

[17] Everllence. 8S60ME-C10.7-GI-HPSCR. 2026.

[18] RINA. HEDY LAMARR - IMO 9498743 2026. https://www.leonardoinfo.com/home/ship/16080/data/generalInfo (accessed February 6, 2026).

[19] Sea-Distance.org. Distance Valencia-Palma 2026. https://sea-distances.org/ (accessed February 6, 2026).

[20] Restrepo RR, Gutierrez AS, Eras JC, Hernandez B, Forero JD. Experimental study of the potential for thermal energy recovery with thermoelectric devices in low displacement diesel engines. Heliyon 2021;7. https://doi.org/10.1016/j.heliyon.2021.e08273.

[21] Naveiro M, Romero Gómez M, Arias-Fernández I, Baaliña Insua Á. Thermodynamic and environmental analyses of a novel closed loop regasification system integrating ORC and CO2 capture in floating storage regasification units. Energy Convers Manag 2022;257. https://doi.org/10.1016/j.enconman.2022.115410.

[22] Herdzik J. Decarbonization of marine fuels—The future of shipping. Energies (Basel) 2021;14:4311.

[23] Vega F, Sanna A, Maroto-Valer MM, Navarrete B, Abad-Correa D. Study of the MEA degradation in a CO2 capture process based on partial oxy-combustion approach. International Journal of Greenhouse Gas Control 2016;54:160–7. https://doi.org/10.1016/j.ijggc.2016.09.007.

[24] Vevelstad SJ, Buvik V, Knuutila HK, Grimstvedt A, Da Silva EF. Important Aspects Regarding the Chemical Stability of Aqueous Amine Solvents for CO2Capture. Ind Eng Chem Res 2022;61:15737–53. https://doi.org/10.1021/acs.iecr.2c02344.

[25] Austgen DM, Rochelle GT, Peng X, Chen CC. Model of vapor-liquid equilibria for aqueous acid gas-alkanolamine systems using the electrolyte-NRTL equation. Ind Eng Chem Res 1989;28:1060–73.

[26] Akhoundi M, Deymi-Dashtebayaz M, Tayyeban E, Khabbazi H. Parametric study and optimization of the precooled Linde–Hampson (PCLH) cycle for six different gases based on energy and exergy analysis. Chemical Papers 2023;77:5343–56. https://doi.org/10.1007/s11696-023-02866-5.

[27] Chen F, Morosuk T. Exergetic and economic evaluation of CO2 liquefaction processes. Energies (Basel) 2021;14:7174. https://doi.org/https://doi.org/10.3390/en14217174.

[28] Peng D-Y, Robinson DB. A new two-constant equation of state. Industrial & Engineering Chemistry Fundamentals 1976;15:59–64.

[29] Aliyon K, Mehrpooya M, Hajinezhad A. Comparison of different CO2 liquefaction processes and exergoeconomic evaluation of integrated CO2 liquefaction and absorption refrigeration system. Energy Convers Manag 2020;211. https://doi.org/10.1016/j.enconman.2020.112752.

[30] Cochran. ST36 Steam Boiler. 2021.

[31] Everllence. GenSet-L23/30DF. 2024.

[32] Lemmon EW, Bell IH, Huber ML, Mclinden MO. REFPROP Documentation Release 10.0. 2023.

[33] Kotas TJ. The exergy method of thermal plant analysis. Paragon Publishing; 2012.

[34] Bejan A, Tsatsaronis G, Moran MJ. Thermal design and optimization. John Wiley & Sons; 1995.

[35] Szargut J. Energy and exergy analysis of the preheating of combustion reactants. Int J Energy Res 1988;12:45–58.

[36] Morris DR, Szargut J. Standard chemical exergy of some elements and compounds on the planet earth. Energy 1986;11:733–55. https://doi.org/https://doi.org/10.1016/0360-5442(86)90013-7.

[37] Szargut J, Morris DR, Steward FR. Exergy analysis of thermal, chemical, and metallurgical processes 1986.

[38] Aspen Technology Inc. Aspen Plus 12.1 2022.

[39] Ship&Bunker. Rotterdam Bunker Prices 2025. https://shipandbunker.com/prices/emea/nwe/nl-rtm-rotterdam#LSMGO (accessed October 28, 2025).